geoconvention
Calgary • Canada • May 7-11 2018

Focal-time estimation: A new method for stratigraphic depth control of induced seismicity

Ronald M Weir, Andrew Poulin, Nadine Igonin and David W. Eaton
Department of Geosciences, University of Calgary

Summary

Focal-time estimation is introduced here as a novel method to obtain robust stratigraphic depth control for induced earthquakes. The method requires Vp and Vs time-depth control from coincident multicomponent seismic data, which is achieved by registration of equivalent P-P and P-S reflections. Event focal depths are initially expressed as the zero-offset focal time (2-way P-P reflection time) and then converted to depth by leveraging the abundance of data and methods available for time-depth conversion of seismic data, such as well ties using synthetic seismograms. Application of this method requires high-quality P- and S-wave picks, which are extrapolated to zero offset. This approach avoids the necessity to build and calibrate a 3-D velocity model for hypocenter location, or the determination of accurate absolute origin times. This method also implicitly accounts for factors that are often ill-constrained for most velocity models, such as transverse isotropy of the medium, since these factors similarly affect both the induced seismicity arrival times and the 3-D seismic data. We apply our new method to an induced seismicity dataset with events up to M3.6, recorded using a shallow well monitoring array in Alberta, Canada. Reconciling the seismic processing datum with the microseismic datum was found to be a critical, but not insurmountable, challenge. The inferred focal depths place events above basement and at or below the treatment depth.

Introduction

In a microseismic survey, data are recorded continuously and later analyzed for seismic events. When a seismic event is recorded on the continuous data stream, it is identified by a compressional event (P wave) followed by a shear (S wave) event. We refer to the P-wave arrival time as Tp, and the S-wave arrival time as Ts. Time 0 for the seismic event (the time of origin) is not generally known. If the Vp and Vs velocity models are known, then the calculated distance from the geophone recorder to the seismic event can be determined. Multicomponent reflection seismic can provide the Vp and Vs information for the study area, and the data can be used to calculate the focal time and depth for microseismic events. Reflection seismic data records two-way travel time, either PP data or PS (converted) data. Microseismic data travels through the same geologic column, but only in one direction. For the simplest case, the PP reflected data recorded to a depth time would be twice the P wave microseismic signal originating from the same depth. Since reflection seismic data is processed to an artificial datum above the highest elevation point, corrections must be applied to reconcile the microseismic and reflection data.

The formation of primary interest in this study is the Devonian age Duvernay, overlain by the Ireton shale, and sits on top of the Swan Hills formation. The Duvernay is drilled and completed using

horizontal drilling and hydraulic fracturing techniques. Numerous microseismic and induced seismic events have been recorded at these depths and are used in this study. The microseismic events are located beneath the 3D, 3C seismic reflection survey.

Theory

In microseismic processing depth is calculated with a velocity model that is calibrated from perforation shots. The method proposed here uses the velocity model derived from the depth-calibrated PP-PS seismic reflection data. Figure 1 illustrates the relationship between reflection seismic data and microseismic recording. This relationship provides a more accurate velocity field since 3D seismic covers a large area, where as the perforation shot only gauges the velocity field from its location. In the PP and PS seismic volumes, we correlated several seismic reflection events both in PP and PS time from the same formations. These events generate Vp/Vs ratios within the entire seismic volume. These values are valid for the reflection data calibrated to a datum above sea level using a certain replacement velocity. Since a datum correction has been applied to the P- and S-wave picks at the microseismic receiver locations, the Vp/Vs ratios of the microseismic events will reflect the seismic. Ts-Tp time grids are calculated for the seismic formations using their PP and PS horizons extracted from the 3D seismic. From these Ts-Tp grids it is then possible to correlate them with the microseismic Ts-Tp times. Since the location of the microseismic events are known with respect to the geological formations in Ts-Tp time, it is relatively simple to interpolate those Ts-Tp times to PP time.

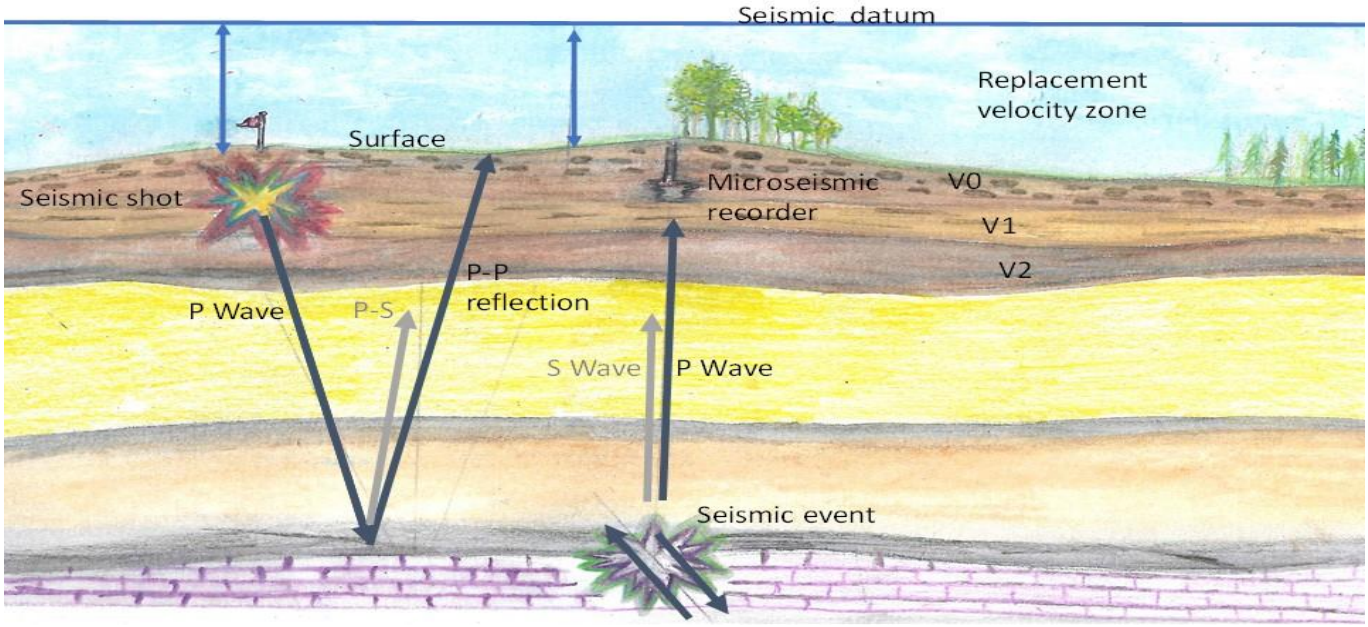

Figure 1. Illustration of the relationship between reflection seismic data and microseismic recording. Reflection seismic data is corrected to an artificial datum, above the highest elevation. The dark arrows represent PP (reflection) and direct P-wave, the gray arrows represent PS (reflection) and direct S-wave (microseismic). The reflection seismic data is time-adjusted downward to match the microseismic data.

Examples

Figure 2 displays a reflection section displaying PP and PS data displayed in PP time after registration. We use the PP and PS reflection data to provide a velocity model to predict the depth to the microseismic events. To do this we must correct the PP and PS seismic data downward to the depth of the microseismic source.

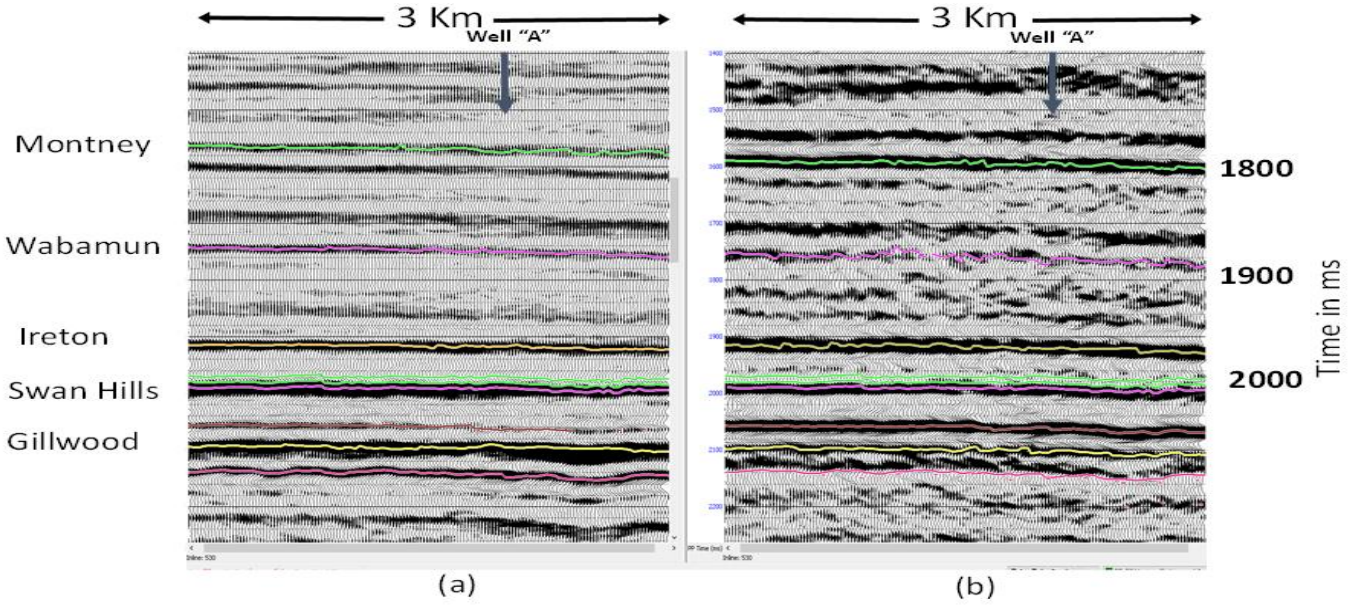

Figure 2. PP (a) and PS (b) seismic data in PP time, showing events used for registration of PP and PS arrival times.

We use the PP two-way reflection data (T) for the Swan Hills seismic event, and the 3D datum of 1100 meters. We then added our datum correction to the buried geophone to bring the data to the same datum as the 3D seismic. The surface elevation of the geophone is 881m ASL, this gives (1100m – 881m) = 219m of material with a replacement velocity of 2900 m/s, this results in a correction of 76ms. The geophone is located 27 meters below surface, with a near surface velocity estimated of 800 m/s, this results in a correction of 38 ms. The total correction that is applied to correct the Tp time at the geophone to datum is 114 ms. In a similar fashion, the Ts time at the microsesimic recorder is corrected to the PS 3D datum using Vp/Vs ratio inferred from the PP / PS registration.

The recorded PP time for the Swan hills formation is 1975 ms. The recorded PS time for the Swan hills formation is 2985 ms. Subtracting the PS time from the PP time gives us the equivalent Ts-Tp time with respect to the 1100 m datum, in this case 1010 ms. We can then apply our datum corrections to the Tp and Ts picks from microseismic source. This results in a Ts –Tp time 1000 ms for the event. This places the event just above the Swan Hills formation (interpreted to be the Duvernay formation). From this we interpolate the Ts-Tp time to PP time; the PP time the values are then converted to TVD. The seismic event arrival times are depth converted using a synthetic seismogram from well "A." The depth to the Base of the Duvernay Formation is 3438 TVD which puts the depth of the Duvernay from the seismic event at 3411m.

Results

For a set of microseismic events with clear arrival-time picks, the PP focal times were determined using the methods outlined above. The event locations are displayed in Figure 3 with the horizon surfaces. The Swan Hills and Ireton markers bracket the Duvernay zone where the injection occurred. The resolved hypocentres show events spanning the interval from the Gilwood to the Ireton, with most events located below the Swan Hills (and therefore, below the Duvernay zone).

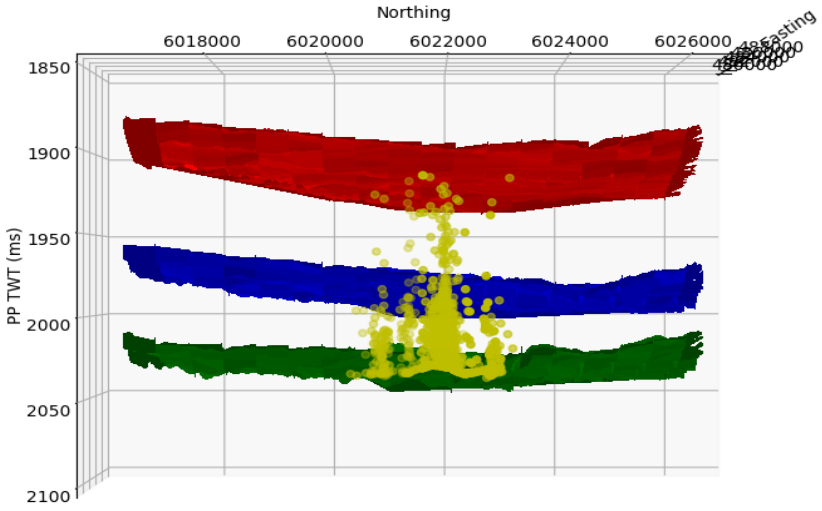

Figure 3 Microseismic events in terms of P-P time plotted against picked horizons Ireton (red), Swan Hills (blue) and Gilwood (green).

Conclusions

This paper outlines a novel focal-time method to achieve stratigraphic depth control for induced seismicity. The method operates in P-P time and integrates arrival time picks from microseismic observations with horizon time picks from multi-component 3D seismic data. This approach resolves some of the uncertainty in determining event focal depths that inevitably arise from incomplete velocity information in 3D (especially in terms of anisotropy parameters) and uncertain time picks for calibration shots. Integration of seismic and microseismic data requires considerable care in the selection of a datum, as the same processing datum must be applied to both sets of measurements to obtain accurate results. We applied this method to coincident microseismic and multi-component 3D data from an area near Fox Creek, Alberta. The resulting inferred focal times place the events between the Gilwood and Ireton formations, which bracket the injection zone. The majority of events cluster at depths below the depth of injection at the Duvernay Formation.

Acknowledgements

The ToC2ME program was enabled by generous support from two companies. Financial support was provided by Chevron and the Natural Sciences and Engineering Research Council of Canada (NSERC) through the NSERC/Chevron Industrial Research Chair in Microseismic System Dynamics. Arcis Seismic Solutions is sincerely thanked for providing the 3D multicomponent seismic data used in this analysis. CGG is thanked for providing software used to display and interpret the data. All sponsors of the Microseismic Industry Consortium are also sincerely thanked for their ongoing support of this initiative.

References

Bao, X., and Eaton, D. W., 2016, Fault activation by hydraulic fracturing in western Canada: Science, page aag2583.

Eaton, D. W., 2018, Passive seismic monitoring of induced seismicity: Fundamental principles and application to energy technologies: Cambridge University Press.

Garotta, R. J., and Grange, P. Y., 1987, Comparison of responses of compressional and converted waves on a gas sand: SEG Technical Program Expanded Abstracts 1987, 627–630.

Lomax, A., Michelini, A., and Curtis, A., 2014, Earthquake location, direct, global-search methods: Encyclopedia of Complexity and Systems Science, 1–33.

Ong, O. N., Schmitt, D. R., Kofman, R. S., and Haug, K., 2016, Static and dynamic pressure sensitivity anisotropy of a calcareous shale: Geophysical Prospecting, 64, no. 4, 875–897.

Schultz, R., Wang, R., Gu, Y. J., Haug, K., and Atkinson, G., 2017, A seismological overview of the induced earthquakes in the Duvernay play near fox creek, Alberta: Journal of Geophysical Research: Solid Earth, 122, no. 1, 492–505.

Zhang, H., Eaton, D. W., Li, G., Liu, Y., and Harrington, R. M., 2016, Discriminating induced seismicity from natural earthquakes using moment tensors and source spectra: Journal of Geophysical Research: Solid Earth, 121, no. 2, 972–993